

Impact of tire and traffic parameters on water pressure in pavement

Fauzia Saeed*, Mujib Rahman¹ and Denis Chamberlain²

Department of Civil and Environmental Engineering, Brunel University London, Kingston Ln, Uxbridge, Middlesex UB8 3PH

ABSTRACT

It is generally believed that, irrespective of pavement type, the water on the pavement surface or water build up in the internal voids, or water pressure through cracks due to traffic action plays a significant role for the functional and structural failure of the pavement. Although extensive studies on water related material degradation have been conducted in the last fifty years, research on measuring water pressure due to dynamic action of load and its impact on pavement performance is very limited. The influence of tire characteristics on asphalt surfaces is also very limited. This study attempts to address the impact of water and tire parameters in the pavement subjected to dynamic loading. The idealised pavement consisted of 100mm concrete slab with 2mm continuous fissure. The concrete pavement was overlaid with 20mm semi permeable asphalt surface to evaluate the influence of asphalt surfaces on the water pressure. The slabs were submerged with 2mm and 4mm water and were subjected to 5kN and 10kN loads applied at 1Hz, 5Hz, 10Hz and 15Hz. The loading plate was designed to simulate new and part worn tires with a square and a square with channel pattern with up to 8mm thickness to represent tread characteristics. It was found that dynamic water pressure increases significantly when high frequency loading combined with square type of tread, and water trapped inside the groove which generates pumping action. The water pressure also increases with thread thickness. Load magnitude and depth of surface water have marginal impact on the water pressure in the pavement.

Author Keywords: pore water pressure; tread pattern; frequency; load, water depth; asphalt, stone mastic asphalt, concrete

*Corresponding author, Department of Civil and Environmental Engineering, Brunel University London UB8 3PH
Fauzia.Saeed@brunel.ac.uk

¹Senior Lecturer, Department of Civil and Environmental Engineering, Brunel University London UB8 3PH
mujib.rahman@brunel.ac.uk

²Visiting Professor, Department of Civil and Environmental Engineering, Brunel University London UB8 3PH
denis.chamberlain@brunel.ac.uk

32 **INTRODUCTION**

33 The adverse impact of water on pavement performance is a well-known concern in the pavement engineering
34 community. Studies on water related distresses are predominantly manifested towards material degradation due
35 to loss of adhesion and/or cohesion of the mixture matrix for asphalt pavement or failure of joints and
36 foundation in concrete pavement. In addition, many modern types of asphalt road surfaces, such as stone mastic
37 asphalt (SMA), thin surfacing or porous asphalt, experience premature failure such as ravelling, leading to
38 pothole and/or other structural failure. It is generally believed that the water on the surface or water build up
39 inside the pavement exacerbates this pressure, which may result in pavement surface layer spalling or loosening,
40 leading to localised and eventually structural damage (Kim *et al.*, 2008; Willway *et al.*, 2008; Karlson, 2005;
41 Lindly, Jay K., Elsayed, Ashraf S., 1995).

42 In asphalt pavement, the water pressure is dependent on tire characteristics (tire pressure, tread shape, depth, and
43 patterns), traffic characteristics (magnitude, speed) as well as mixture configurations such as size and gradation
44 of aggregate, void content and level of compaction. For example, in dense and close graded surface course
45 (voids less 4%), the water infiltration is relatively low and slow, whereas water drains freely in high void
46 content mixtures such as in porous asphalt. Uniformly graded mix with intermediate void content, 6%-12%,
47 may experience water infiltration and water storage within the mixture. In addition, water may also pass through
48 cracks or blocked interconnected voids caused by debris, and creates capillary force at the interface when
49 subjected traffic, which may eventually be damaging to interconnected bonds by adhesion failure. In concrete
50 pavement, water infiltration through crack/joints can lead to water pressure generated at the bottom of the slab
51 when traffic passes through the water-filled crack/joint. This can potentially lead to under slab voiding and poor
52 load transfer efficiency of the joints/crack (Mathavan, S., Rahman, M., Martyn Stone-Cliffe Jones., 2014).

53 In the available literature on water pressure in pavement, most studies are found to be computational and/or
54 analytical. Experimental studies are extremely limited. This is primarily due to the complexity of measuring
55 water pressure under traffic load in the laboratory environment as well as in the field condition. This study
56 therefore, concentrates on developing a laboratory test to measure water pressure under a repeated vertical load
57 when pavement surface is subjected to flooding with various depth of water. The effect of load magnitude, load
58 frequency, tire tread shape, and patterns, and depth of water on the surface are investigated. This paper covers
59 two aspects of water related issues in asphalt pavement. In the first section, a brief overview of previous studies
60 together with tire tread characteristics and the concept of tire-water-pavement interaction are reviewed. The
61 second part describes the test set-up and presents the influence of tread pattern and depth, load frequency and

62 load magnitude on pore water pressure on two idealised pavement structures. Finally, key conclusions are
63 presented.

64 **PAST STUDIES ON WATER PRESSURE MEASUREMENT IN PAVEMENT**

65 Xiaoyong (2008) developed a theoretical model whereby the asphalt pavement was regarded as an axially
66 symmetrical body of multi-layered saturation elastic half space(Cui<i> et al.</i>, 2009)(Cui<i> et al.</i>,
67 2009)(Cui<i> et al.</i>, 2009). The pore water pressure in asphalt pavement under mobile load was calculated.

68 The results demonstrated that the pore water pressure in the internal asphalt pavement has a close relation to the
69 permeation coefficient of surface, surface thickness, wheel speed and material parameters. The pore pressure at
70 the interface between surface layers and the base layer of the asphalt pavement is maximized when the pore of
71 pavement is entirely saturated, under the loading action. Under the repeated action of loading, the pavement
72 fatigue cracking may happen, a process which accelerates the development of the cracking of asphalt pavement.

73 Li and Sheng (2012) applied the finite element method built on the porous elastic theory to replicate the pore
74 water pressure produced in the base layer of rigid pavement under the vehicle load. They stated that the
75 maximum pore pressure is created in the middle depth of the base layer. The pore water pressure of this position
76 is investigated to evaluate the base layer performance under different vehicle speeds, the difference between
77 pore water pressure when vehicles speed is 10m/s and 60 m/s is 1.91 kPa. The numerical simulation results
78 indicated that the dissipation time decreases with increasing vehicle speed, 1.04s at 60 m/s and 1.37s at 10 m/s.

79 The results also displayed that the high vehicle speed has a high impact on base erosion (Li and Sheng 2012).
80 Other method such as the Finite Difference Method (FDM) and the Biot Dynamic Consolidation Theory were
81 applied to investigate the dynamic response of the saturated asphalt pavement, the results demonstrated that the

82 positive pore water pressure under wheel is associated with pumping action. However, the negative pressure
83 refers to the suction in pavement surface where water is sucked cyclically under traffic loading. This suction
84 increases with vehicle speed leading to increase dynamic pore water pressure (Cui et al. 2009) . A three-

85 dimensional fluid flow model was built on Lattice Boltzmann to study the unsteady dynamic fluid flow in
86 asphalt pavements (Kutay and Aydilek 2007). This study investigated samples with different hydraulic
87 conductivity resulting from aggregate angularities, orientations and fine distribution. Taking into account these
88 samples have the same nominal size of aggregate and same compaction energy. It is stated that dynamic fluid
89 pressure influences the moisture transport inside the asphalt concrete.

90 There are a limited number of studies found in the literature that have experimentally tried to measure and
91 evaluate the impact of water pressure in the overall pavement structure. The experimental study by Jiang *et al* ,

92 (2013) generated dynamic water pressure in a cylindrical asphalt concrete specimen by compressed air, the
93 specimen base wrapped with epoxy resin glue to orient the flow of water through voids in the specimen into an
94 established space. It was stated that dynamic water pressure on asphalt surface depends on the load magnitude.
95 Jiang *et al* (2013) also reported that the excess water pressure decreases the frictional strength of the structural
96 part of the road and foundation materials by generating buoyancy inside these materials (Cook and Dykins
97 1991; Kutay and Aydilek 2007). Excess pore water pressure can be formed inside the subgrade and pavement
98 structural components by tire influences (Ridgeway 1982).
99 Yuan and Nazarian (2003) demonstrated from laboratory and in situ investigations that moisture content has
100 significant negative impact on road base and subgrade materials. Since the pavement ability to transmit dynamic
101 loads is forced by traffic, the performance can be greatly deteriorated because of deterioration of foundation
102 support (Moulton 1980). The movement of the wheel on the asphalt pavement with a saturated subgrade can
103 generate a moving pressure wave that in turn can produce large hydrostatic forces inside the structural section.
104 The specific aspects of pulsating pore pressure considerably influence the load carrying capacity of the whole
105 structural component of the flexible pavement (Cedergren et al. 1973). These conditions can create excessive
106 deflection, cracking, decrease in the load carrying capacity, ravelling and disintegration of asphalt mixes,
107 subgrade instability, pumping, and loss of support (Lindly and Elsayed 1995; Flynn 1991). However, none of
108 the previous research systematically investigated the impact tire characteristics during dynamic loading on the
109 pore pressure in the asphalt surface.

110

111 **TIRE TREAD CHARACTERISTICS**

112 Tires with different tread designs are used for controlling the noise, providing good traction in wet condition and
113 ensuring a comfortable ride for various driving styles. There are four primary types of tire tread, namely,
114 symmetrical, directional, asymmetrical, and directional asymmetrical these characterised by the geometrical
115 shape of the grooves, ribs, sipes, dimples, blocks and shoulder as shown in **Figure 1**.

116

117 **Figure 1. Schematic diagram of tread pattern based on the geometrical shape of the tread component**

118

119 The detail explanation of each tire type, advantage, and limitations can be found in the literature (Heisler 2002;
120 Hanson et al. 2004; Gent and Walter 2006; Bodziak 2008; McDonald 1992). It is evident that the actual tread
121 shape and pattern in real tire is complex, however, most tires tread have two general characteristics in common.

122 The first one is a channel to remove water quickly from the contact area (act like a water channel to avoid aqua
123 planning) and the second one is a rain groove (voids to ensure traction) to pump water out from under the tire by
124 the action of the tread flexing. However, under dynamic loading, the characteristics of these elements interact
125 and there is a combination of pumping, and splashing happen at the same time. A conceptual explanation is
126 given in the following section.

127

128

129 **CONCEPT OF TIRE-WATER-PAVEMENT INTERACTION**

130 When water enters the asphalt surface, it creates hydrostatics pressure due to the action of moving vehicles. The
131 magnitude of pressure varies, depending on the surface type, tire tread depth and presences of existing distresses
132 on the surface. The conceptual illustration of tire-water-pavement interaction is shown in Figure 2.

133

134 **Figure 2. Conceptual illustration of tire-water-pavement interaction**

135

136 The interaction of tire pavement can be divided into 3 zones when rolling on a wet surface (Cerezo et al. 2014)
137 zone 1 is the major part to drain the stagnant water film covering the road surface, and this part depends on the
138 water depth, the speed, tire tread depth and the road surface macrotecture. With increasing speed and water
139 depth, it will be more difficult to drain the water from the road surface, thus creating a possible scenario for
140 water infiltration and moisture damage. However, with the help of tread depths this can be minimized. After
141 pass through the zone 1, the remaining water on the surface goes to zone 2, or middle zone and this zone is
142 responsible for the final removal of water, this assisted by sipes and grooves along the contact patch. The
143 squeezing of water on zone 2 will dissipate the remained fluid to all directions; especially to beneath the tread
144 blocks and ribs, and this pressure may cause further infiltration in pavement. The water film in zone 3 has
145 almost completely been squeezed out, so in this region the contact between the tire and pavement start, to
146 happen.

147 The prone zones to develop water infiltration and overpressure on micro voids (**Figure 2**) are 1 and 2 because in
148 these areas the amount of water still high and not totally dissipated. Thus, in roads with cracks, the possibility to
149 create moisture damage problems is higher than new roads because of distresses already present on the surface.

150 The water is a relatively difficult fluid to drainage when compared with air for example Dixon (1996). The
151 density of water is approximately 999.2 kg/m^3 and viscosity is $1.14 \times 10^{-3} \text{ Ns/m}^2$. Therefore, the water after being

152 squeezed out from the longitudinal channels will be directed sideways to help drainage. Dixon (1996)
153 demonstrates a “drainage” number to explain the problem with water drainage through the tread channels. It is a
154 non-dimensional measure and correlates the cross-sectional area of the channel in front view, divided by the
155 cross-sectional area of the approaching water. According to this, if the number is greater than 1.0, the channels
156 will be sufficient to drain the water, however if the number is less than 1.0, the tire will need the help of lateral
157 drainage to provide good flow of water. The time of the contact of the tire is extremely important as well, for
158 example, if the car is at in high speed it will be more difficult to drain the water compared with slow speed.
159 According to Dixon (1996) the time that the rubber contacts with the footprint is normally 6ms at a speed of
160 30m/s and the water will be drained in only 2 or 3ms.

161

162 **EXPERIMENTAL PROGRAMME**

163 An investigation has been conducted to study the influence of tread depth, tread pattern, loading range and
164 frequency range and water depth on the magnitude of water pressure under dynamic loading. It should be noted
165 that simulating tire pavement interaction and related water pressure accurately in real pavement and even in the
166 laboratory environment is extremely difficult due to the complexity of tire interaction with the pavement
167 structure, material and influence of other factors such as layer deboning, vehicle speed, tread shape and pattern,
168 for example. The primary aim of this study was therefore to evaluate how tire parameters influence water
169 pressure in an idealised situation (simplistic pavement structure). Careful considerations were given when
170 selecting load platen, tread characterises and test parameters. A brief explanation of loading platen and
171 experimental set-up is given in the following sections.

172

173 **Loading platen, tread pattern and tread depth**

174 A picture of the custom build loading device and rubber pad to represent idealised tread pattern and tread depth
175 used in the experiment is shown in **Figure 3**. The concept was adopted from earlier work by Rahman and Thom
176 (2012). The dimension of the loading device (as shown in Figure 3a) was based on the concept that a truck tire
177 patch is approximately 300 mm in diameter, so this was scaled down three times to 100mm. A 12mm rubber pad
178 with different tread pattern and thickness (as given below), to simulate tire characteristics, was attached to the
179 loading platen by adhesive.

180

- 181 • Tread pattern: a squared box (SQ) to represent Sipes, groove and dimple of the tire and a square box with a
182 channel (SL) to represent block and ribs of the tire and non-treaded tires (NT).
- 183 • Tread depth: 8mm tread depth to represent new tire, 3mm to represent part worn tire and 1.5mm to
184 represent worn tire.

185
186 **Figure 3a)** 100mm X100mm loading head

187 **Figure 3b)** Rubber pad representing tread pattern and shape

188 **Figure. 3. Loading device**

189 **Idealised pavement**

190 The idealised structure was adopted to represent two scenarios in pavement construction.

191 Scenario 1: Figure 4a represents an idealised concrete pavement, for which a 40mm rubber pad was used to
192 represent the pavement foundation.

193

194 **Figure 4a.** Idealised pavement

195

196 Scenario 2: Figure 4b represents an idealised asphalt pavement. A 100mm concrete slab was to represent the
197 asphalt concrete and base layers and a 40mm rubber pad to represent the pavement foundation. The concrete
198 slab eliminates the possibility of water infiltration to a lower layer, which would be the case with an asphalt
199 binder layer.

200

201 **Figure 4b:** Idealised pavement with asphalt overlay

202 ***Test Set-up***

203 Two C40 concrete slabs (300mm x 300mm x 100mm C40 concrete slabs) were manufactured. The slab has a
204 150mm x 150mm x 20mm deep recess at the middle. Preliminary study was carried out to measure pore water
205 pressure in eight pore holes under the loading patch, by using manometer (Saeed 2015). The test results showed
206 that maximum pressure is generated at the central pore hole. Therefore, it was decided to use single pore hole
207 measurement. As this study is mainly to evaluate the impact of tire characterises and loading frequencies on
208 water pressure, the distribution under the contact patch was not included. Future study will address this.

209

210 A 2mm pore hole was created at the centre of the recess to representative a continuous void through the depth.

211 The 2mm void size was the minimum practical size possible to manufacture in the laboratory. In addition, full

212 depth continuous pore was chosen to simplify the crack pattern and evaluate the influence of a full depth crack
213 when water passed through this under dynamic loading when the surface is flooded with water. The test setup
214 for both scenario 1 and scenario 2 are given in Figure 5.

215

216 In scenario 1, the recess area in concrete surface was filled with water to simulate water pressure under the slab
217 when water is forced through a narrow crack (2mm) during traffic loading. This scenario is also used to test
218 experimental setup for its consistency and repeatability of the test.

219

220 **Figure 5a:** Scenario No. 1

221 **Figure 5b:** Scenario No. 2

222 **Figure 5 Schematic diagrams of test scenarios**

223

224 The purpose of scenario 2 is to evaluate the impact of a 20mm semi permeable asphalt surface laid on the same
225 100mm concrete slab with 2mm wide full depth crack. 20mm asphalt surface was chosen to maintain the overall
226 thickness of the concrete slab to 100mm. In addition, this also represents various thin surfacing system used for
227 asphalt overlay in urban and rural highways (Highways England 2012). The average texture of the asphalt
228 surface was measured as 1.27mm. The asphalt surface was saturated to minimise the impact of surface texture
229 and maximise the effect of internal voids. The concrete slab was used in the idealised pavement structure to
230 simulate the lower layers of asphalt (binder and base). The impermeable concrete slab eliminates the
231 complication of water saturation in lower asphalt layers, which could potentially influence the water pressure.

232

233 *Data acquisition*

234 The lower end of the pore void, at the bottom of the slab, was connected to a pressure sensor, capable of
235 measuring low pressures in the 0-7 kPa range. The sensor range was based on the preliminary trials using a
236 manometer to determine water pressure for 1Hz loading frequency. The sensors were connected to high-
237 accuracy fast data acquisition device with 100 Hz sampling rate. The sensor electrical output ranges from 0-16.7
238 mV/V for pressure in range of 0- 6.89476 kPa. The sensor employed in this study excludes atmospheric pressure
239 (101kPa). The test set-up is shown in **Figure 6**.

240

241

Figure 6. Experimental set-up

242 The testing was conducted using an INSTRON 8501 servo-hydraulic testing rig, capable of applying loads at
243 0.1Hz to 50Hz in the 1kN to 100 kN load range. Testing was operated in a controlled load/stress mode. The test
244 consists of running the equipment at a required load for a given frequency and water depth, recording the
245 resulting amplitude of water pressure under slab. By repeating the test on each tread enables the influence of
246 tread shapes to be evaluated. Figure 7 shows an example of the load pulse at applied loads 5kN and 10kN at
247 1Hz and the corresponding water pressure under the slab. There are some variations in the water pressure
248 measurement. This was due to the difficulty of maintaining constant level of surface water during load
249 application. Each test case was repeated for three times, and the results found to be within 5% agreement.

250

251 **Figure 7a)** Applied load 5kN at 1 Hz

252 **Figure 7b)** Pore water pressure at 5 kN at 1 Hz and tread 8SQ4

253 **Figure 7c)** Applied load 10kN at 1 Hz

254 **Figure 7d)** Pore water pressure at 10 kN at 1 Hz and tread 3SQ4

255

256 **Figure 7. Typical signals at different loading frequencies is shown in 5KN, 10KN and frequency 1Hz**

257

258 **TEST SPECIFICATIONS**

259 The test specifications are shown in Table 1. A constant feed of water was supplied to maintain a specific water
260 depth during testing. It should be noted that the depth of water was difficult to maintain, especially at high
261 frequency due to significant splashing after each load pulse. Research is underway for a mechanical feed of
262 water. The applied loads were chosen to as 5kN and 10kN to simulate light and heavy vehicle loading.

263

264 **TABLE 1 Test specifications**

265

266 In total 112 cases had been tested (7 tread shape, 2 loads, 2 water depth and 4 frequencies). Each test was named
267 as 8SQ4, which refers to 8mm tread depth, square tread pattern and 4mm water depth and so on. Each case was
268 tested at 5kN and 10kN and at 1 Hz, 5Hz, 10Hz and 15Hz, and was repeated for three times. This means 336
269 tests had been conducted. It should be noted that testing at very high frequency (25 or 50Hz) was found unsafe
270 and maintaining water depth was extremely difficult in the current set-up. However, further works are underway
271 to address this.

272 **RESULTS AND ANALYSIS**

273 The data are analysed to evaluate the influence of load magnitude and frequency, tread patterns and depth on the
274 pore water pressure through a 2mm pore extended through the depth of the slab. The test results on average
275 water pressure against tire characteristics are shown in Figures 8a-8d for scenario 1 and Figures 8e-8h for
276 scenario 2.

277 **Figure. 8a.** 4mm surface water, load 5kN, no asphalt surface

278 **Figure. 8b.** 2mm surface water, 5 kN load, no asphalt surface

279 **Figure. 8c.** 4mm surface water, 10kN load, no asphalt surface

280 **Figure. 8d.** 2mm surface water, 10kN load, no asphalt surface

281 **Figure. 8e.** 4mm surface water, 5kN load, with 20mm asphalt surface

282 **Figure. 8f.** 2mm surface water, 5kN load, with 20mm asphalt surface

283 **Figure. 8g.** 4mm surface water, 10kN load, with 20mm asphalt surface

284 **Figure. 8h.** 2mm surface water, 10kN load, with 20mm asphalt surface

285

286 ***Influence of tread shape and pattern***

287 In general, at a specific frequency, irrespective of applied load, the maximum water pressure was occurred with
288 the 8mm square tread (8SQ4) whilst the pressure decreases with decreasing tread depth, reaching minimum at
289 the no tread situation. It is interesting to note that the water pressure in the zero-tread scenario is the minimum
290 and no change happens despite increasing either load frequency or load magnitude.

291 ***Influence of loading frequency***

292 Irrespective of surface water depth and load magnitude, the water pressure increases with increasing frequency.
293 The water pressure decreases as tread depth decreases. As expected, for a specific frequency, water pressure is
294 higher in a square tread than slot cut tread shape as more water is possible to drain out during the load pulse. It
295 is interesting to note that irrespective of loading frequency, change in water pressure on flat loading plate; i.e. no
296 tread depth.

297 ***Influence of depth of surface water***

298 The depth of surface water, 2mm and 4mm, appears to have only marginal impact on the water pressure
299 (Figures 8a, 8d). The slight increase was observed at high frequency, whereas the changes is negligible at low
300 frequencies.

301 *Load magnitude*

302 As with surface water, the magnitude of load appears to have only marginal influence on the pore water pressure
303 at in all tread shape, tread patterns and loading frequency, showing only marginal increase (3%-10%) between
304 5kN and 10 kN load and between 4mm and 2mm depth of surface water.

305

306 **DISCUSSION**

307 *Influence of tire and load parameters*

308 The worst-case scenario was found to be high loading frequency, when water is trapped in a deep groove (8mm
309 in this) of the tire. The tread depth in a new truck tire could be as deep as 15mm, which may increase pore water
310 pressure significantly.

311 It should be noted that, overall, in the worst-case scenario (8mm square tread 8SQ4, 15 Hz frequency),
312 maximum pore water pressure in this test was approximately 7kPa at the bottom of the slab, which equates to
313 approximately 3%-1.5% of the actual contact stress 3kPa (5000/150²) and 1.5kPa (10000/150²) respectively. To
314 extrapolate this to high speed traffic, the following equation developed by Brown (1974) was utilised.

315

316
$$\log(t) = 0.5d - 0.2 - 0.94\log(v)$$

317

318 Where, t = loading time (sec); d = pavement depth (m), 0.1m slab thickness; and v = vehicle speed (km/h). f

319 (Hz)=1/t (NCHRP, 2004).

320 Brown's equation relates to loading time to vehicle speed and pavement depth profile. The loading time was
321 considered as the average of the pulse times of the stresses in three directions as obtained from the elastic
322 layered theory (Brown 1974). The extrapolated graph relating to water pressure and vehicle speed is shown in
323 Figure 9.

324 **Figure 9.** Extrapolated relation between water pressure and vehicle speed

325

326 It can be seen that at 100 km/hr (~60 mph), the water pressure can be around 28 kPa, which is approximately
327 8% of the applied pressure. Although this is unlikely to create any immediate damage to the road, repeated
328 action of the load will eventually lead to bond deterioration in the mixture matrix and at interface between two
329 layers. The resulted outcome could be stripping at the bottom of the layer and eventual cracking at the road

330 surface and deterioration to foundation. Another point to note is that if the pore opening reduced from 2mm to
331 1mm, the pressure will increase significantly due to capillary action of the water.

332

333 ***Reduction of water pressure due to asphalt surface***

334 A comparison between two scenarios at 5kN applied load on 4mm surface water is shown in Figure 10.
335 Depending on the loading frequency and tread shape and pattern, reduction of approximately 5% to 38%
336 maximum water pressure was measured when concrete slab was overlaid with a semi permeable 20mm SMA
337 asphalt. This reduction could be due to texture in the surface and water storage in side mixture matrix. The tread
338 shape & thickness and frequencies are the main contributory factors for changes in water pressure. The load
339 magnitude, as with scenario 1, has only marginal effect. It is interesting to note that, in the case of no tread case
340 (NT4), the pressure at 15Hz was slightly higher in scenario 2 (Figures 8e-8h) than scenario 1 (8a-8d). It can be
341 due to water build up in the interconnected voids forcing water through the cracks.

342

343 **Figure 10.** Comparison of water pressure at different frequencies on pavement with and without asphalt surface.

344

345 **SUMMARY AND CONCLUSIONS**

346 Water infiltration through a discontinuity (crack/joint) in a pavement generates water pressure at the end of the
347 discontinuity under traffic load. If this discontinuity extends to the full depth, the generated water pressure can
348 lead to deterioration to foundation material, which ultimately can create under stab voids resulting poor load
349 transfer efficiency and failure of the pavement. A novel laboratory test has been developed to measure water
350 pressure underneath a flooded concrete slab that contains 2mm continuous pore (cracks) across the full depth.
351 The test was repeated on a slab overlaid with 20mm semi permeable asphalt surface. The slab was subjected to
352 flooding with 2mm and 4mm water and dynamic compression load of a 5kN and 10kN with three tire patterns
353 (square groove, square channel and no tread) and four tread depths (8mm, 3mm , 1.5mm and 0mm). The load
354 was applied at four different frequencies, 1Hz, 5Hz, 10Hz and 15 Hz.

355 The key conclusions are listed below;

- 356
- Increasing load frequency increases pore water pressure in the pavement. However, water pressure
357 increases significantly when high frequency loading combined with square types of tread with deep
358 tread depth, when water trapped inside the groove. Square tread with channel allows water to drain,
359 which reduces pore water pressure.

- 360
- Irrespective of tread pattern, 8mm tread thickness showed highest amount of water pressure, but the pressure reduces significantly in 1.5mm tread thickness.
- 361
- 362
- Load magnitude has marginal impact on the pore water pressure. The water pressure difference between 5kN and 10kN load was found only between 3% to 10% in all tread patterns, thicknesses and loading frequencies. Similarly, the depth of surface water appears to have minimum impact on the water pressure. It is likely that pore water pressure will build up if pores are filled with water and there is minimum amount of water on the surface.
- 363
- 364
- 365
- 366
- 367
- The asphalt surface can mitigate water pressure underneath the pavement between 5% to 38% depending on the vehicle speed, tread patterns and thickness. This large variation also indicates that, for given surface type, the tire characteristics and vehicles speed will have influence on the pore water pressure.
- 368
- 369
- 370
- 371
- Whilst the magnitude of water pressure is only around 8% of the contact pressure, smaller but continuous voids can significantly increase this pressure, which eventually can lead to degradation of foundation material and progressive deterioration to asphalt surface resulting raveling or stripping.
- 372
- 373
- 374
- Although this study has been conducted on idealised condition, the results showed good repeatability. The results are analogous to limited previous studies available. Further works are underway to measure water pressure at various depths, and asphalt surface with various texture and void characterises. Furthermore, to a great extent, the approach to the research is ad hoc, with no relevant standard approach to measure water pressure in the pavement is existing. In the on-going investigations, a standard test set up is being determined, with use of multiple sensors across the contact patch that will facilitate statistical analysis of experimental data.
- 375
- 376
- 377
- 378
- 379
- 380

381

382 REFERENCE

383

384 Bodziak, W. J. (2008). *Tire Tread and tire Track Evidence: Recovery and Forensic Examination*. CRC Press.

385 Brown, S. F. (1973). "Determination of Young's modulus for bituminous materials in pavement design."

386 *Highway Research Record*.431, Highway Research Board, Washington, D.C., 38–49.

387 Cedergren, H. R., Arman, J. A., and O'Brien, K. H. (1973). "Development of guidelines for design of subsurface

388 drainage systems for highway structural sections." "FHWA-RD-73-14, Federal Highway Administration,

389 Washington, DC.

390 Cerezo, V., Do, M. T., Prevost, D., and Bouteldja, M. (2014). "Friction/water depth relationship—in situ

391 observations and its integration in tire/road friction models." *Proc.Inst.Mech.Eng.Part J*, 228(11), 1285-1297.

- 392 Cui, X.-z., Cao, W.-d., Liu, S.-t., Dong, L.-l., 2009. "On dynamic pore pressure in moisture damage of asphalt
393 pavement". In: GeoHunan International Conference: Challenges and Recent Advances in Pavement
394 Technologies and Transportation Geotechnics.
- 395 Dixon, J. C. (1996). Tires, suspension and handling, 2nd Ed., Society of Automotive Engineers, Warrendale, Pa.
- 396 Flynn, L. Open-Graded Base May Lengthen Pavement Life. *Roads and Bridges*, Sept. 1991, pp. 33-42.
- 397 Gent, A. N., and Walter, J. D. (2006). The pneumatic tire, U.S. Dept. of Transportation, National Highway
398 Traffic Safety Administration, Washington, DC.
- 399 Hanson DI, James RS, NeSmith C. (2004) Tire/pavement noise study. NCAT (National Center for Asphalt
400 Technology) report 04-02, Auburn.
- 401 Heisler, H., (2002). *Advanced Vehicle Technology*. 2nd ed. London: Butterworth Heinemann.
- 402 Jiang, W., Zhang, X., and Li, Z. (2013). "Simulation test of the dynamic water pressure of asphalt concrete."
403 *Journal of Highway and Transportation Research and Development (English Edition)*, 7(1), 23-27.
- 404 Karlson, T. K. (2005). "Evaluation of cyclic pore pressure induced moisture damage in asphalt pavement." M.S.
405 thesis, Univ. of Florida, Gainesville, FL.
- 406 Kim, Y. R., Lutfi, J. S., Bhasin, A., and Little, N. D. (2008). "Evaluation of moisture damage mechanisms and
407 effects of hydrated lime in asphalt mixtures through measurements of mixture component properties and
408 performance testing." *J. Mater. Civ. Eng.*, 20(10), 659–667.
- 409 Kutay, M. E., Aydilek, A. H., Masad, E., and Harman, T. (2007). "Computational and experimental evaluation
410 of hydraulic conductivity anisotropy in hot-mix asphalt." *Int. J. Pavement Eng.*, 8(1), 29–43.
- 411 Li, H. & Sheng, Y., (2012). "Study on vehicle speed in Pore Water Pressure of Rigid Pavement Base using
412 Poro-elasticity". *Applied Mechanics and Materials*, 178(191), 2615-2618.
- 413 Lindly, J. K., and Elsayed, A. S. (1995). "Estimating permeability of asphalt-treated bases". *Transportation
414 Research Record*. 1492, Transportation Research Board, National Research Council, Washington, D.C. 103–
415 111.
- 416 Mathavan. S, M. Rahman and Martyn Stone-Cliffe Jones. (2014) "A Self-Organising Map Classification of
417 Falling Weight Deflectometer Data for Doweled Unreinforced Concrete Pavement Joints", *International Journal
418 of Pavement Research and Technology*
- 419 McDonald, P. (1992). *Tire imprint evidence*. CRC Press.
- 420 Moulton, L. K. (1980). Highway subdrainage design manual; Rep. No. FHWA-TS-80-224. Federal Highway
421 Administration (FHWA), McLean, Va.
- 422 National Cooperative Highway Research Program, NCHRP Project 9-29 AMPT Interlaboratory Study Findings,
423 NCHRP, Washington, D.C., 2004.
- 424 Rahman, M., & Thom, N. (2013). Performance of asphalt patch repairs, Institution of Civil Engineers, One
425 Great George Street, London, UK.
- 426 Ridgeway, H. H. (1982). "Pavement subsurface drainage system." NCHRP Synthesis of Highway Practice 96,
427 Transportation Research Board, National Research Council, Washington, D.C.
- 428 Saeed, F., (2015). "Impact of tire and traffic parameters on water pressure in pavement." Rep. No. 1st year
429 progress report, Brunel University, London.

430 Willway, T., Baldachin, L., Reeves, S., Harding, M. (2008). "The effects of climate change on highway
 431 pavements and how to minimise them": Technical report. Transport Research Laboratory (TRL), Wokingham,
 432 Berkshire, U.K.

433 Xiaoyong, L. Z. D. (2008). "Axial symmetric elastic solution of pore water pressure in asphalt pavement under
 434 mobile load [J]." Journal of Southeast University (Natural Science Edition), 5 014.

435 Yuan, D., and Nazarian, S. (2003). "Variation in moduli of base and subgrade with moisture." *Transportation*
 436 *Research Board 82nd Annual Meeting.*

437

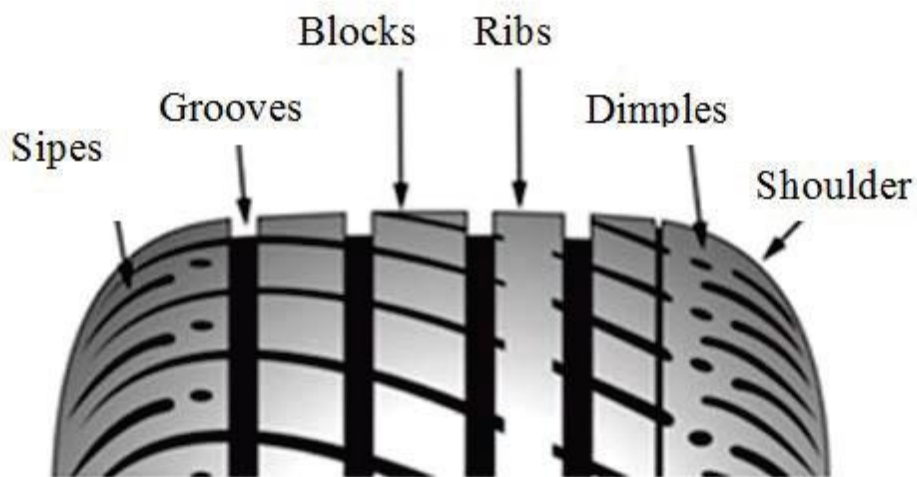
438 **TABLE 1 Test specifications**

439

Variable	Specifications
Surface water depth (mm)	2, 4
Tire Tread Type	Square, Slot, No tread
Tread Depth	0, 1.5, 3 and 8mm
Load (KN)	5, 10
Loading Frequency (Hz)	1, 5, 10 and 15
Type of Load	Dynamic compression
Load Duration (Sec)	0.67-10
Sampling Rate	100 Hz

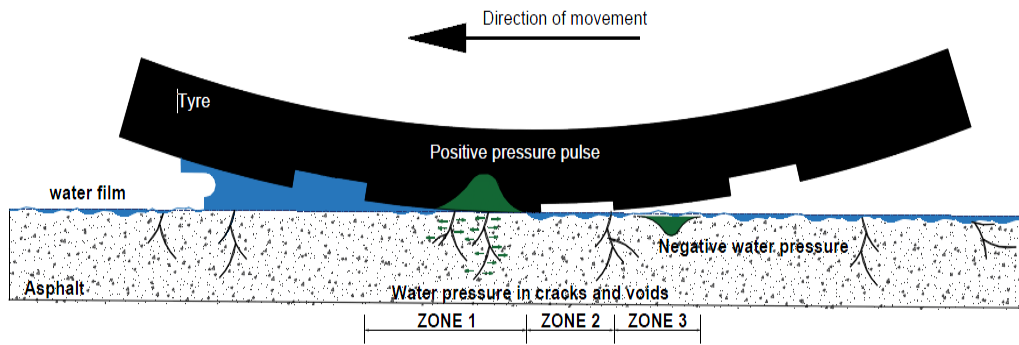
447

448



449

450 **Figure1.** Schematic diagram of tread pattern based on the geometrical shape of the tread component

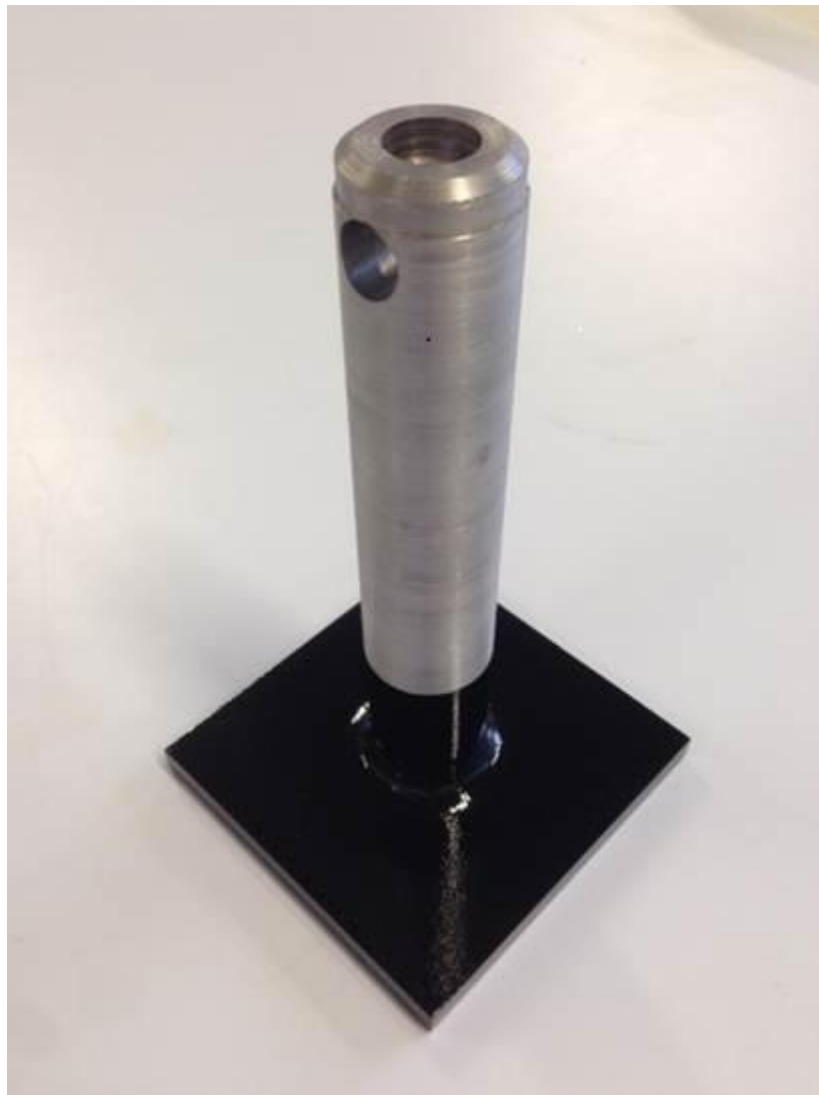


451

452

453

Figure 2. Conceptual illustration of tyre-water-pavement interaction

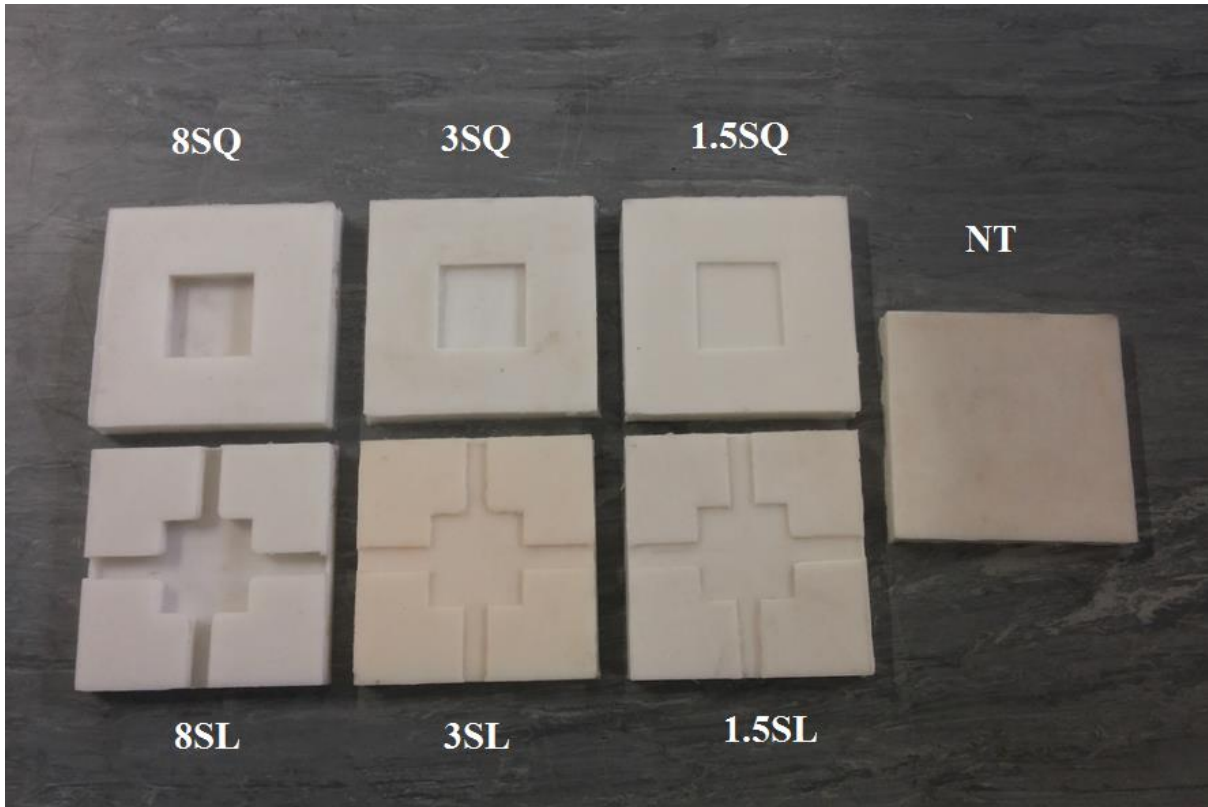


454

455

456

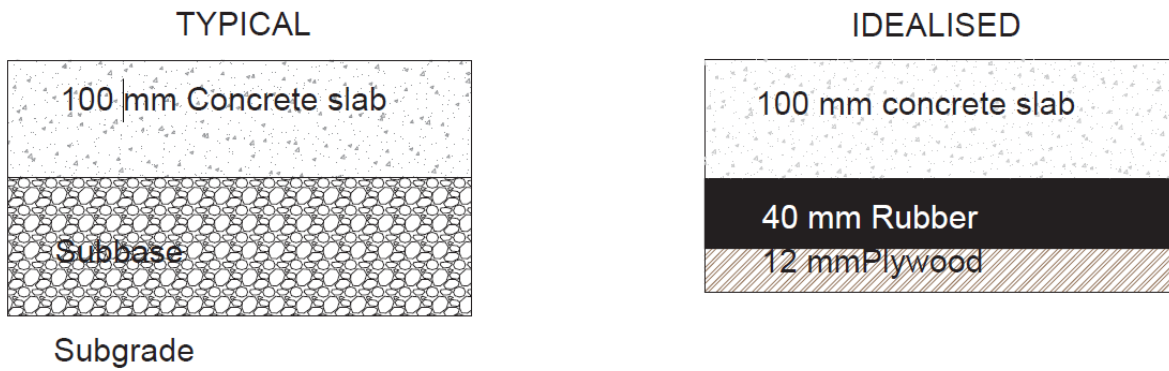
Figure 3a. 100mm X100mm loading head



457
458
459

Figure 3b. Rubber pad representing treads pattern and shape

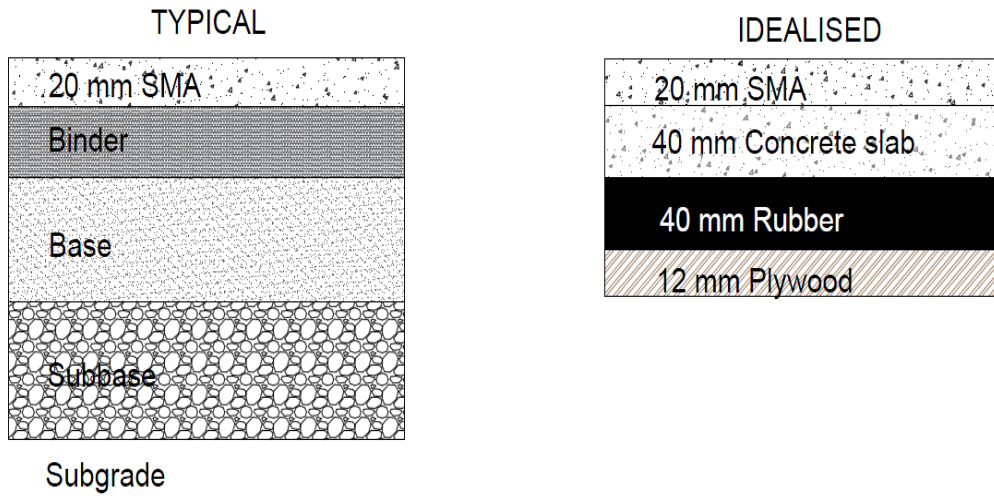
SCENARIO 1



460
461
462
463

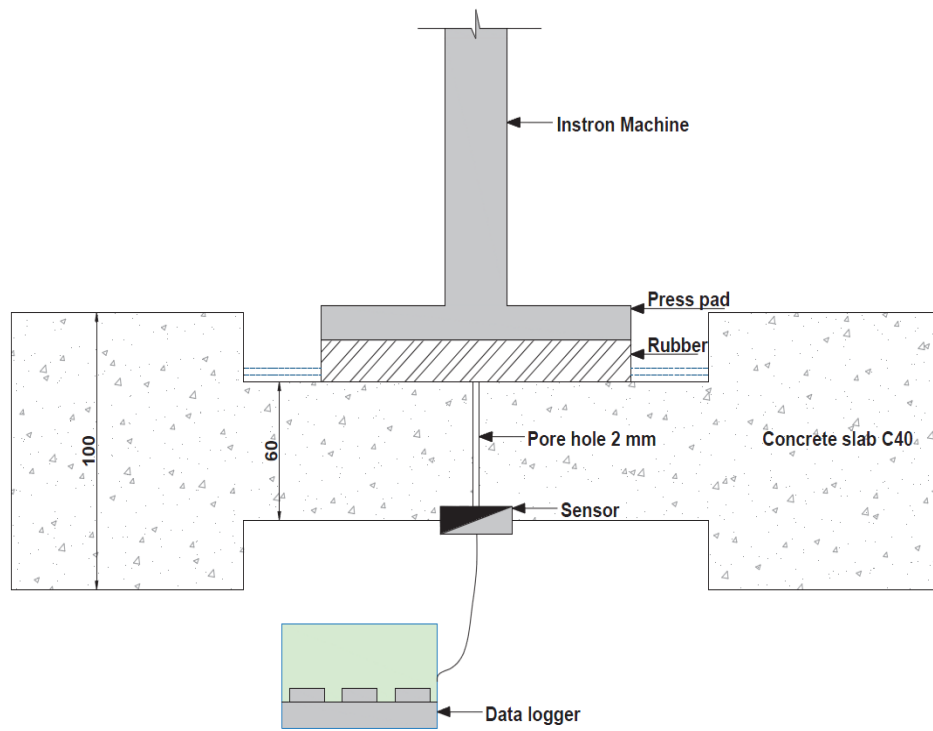
Figure 4a. Idealised pavement

SCNERIO 2



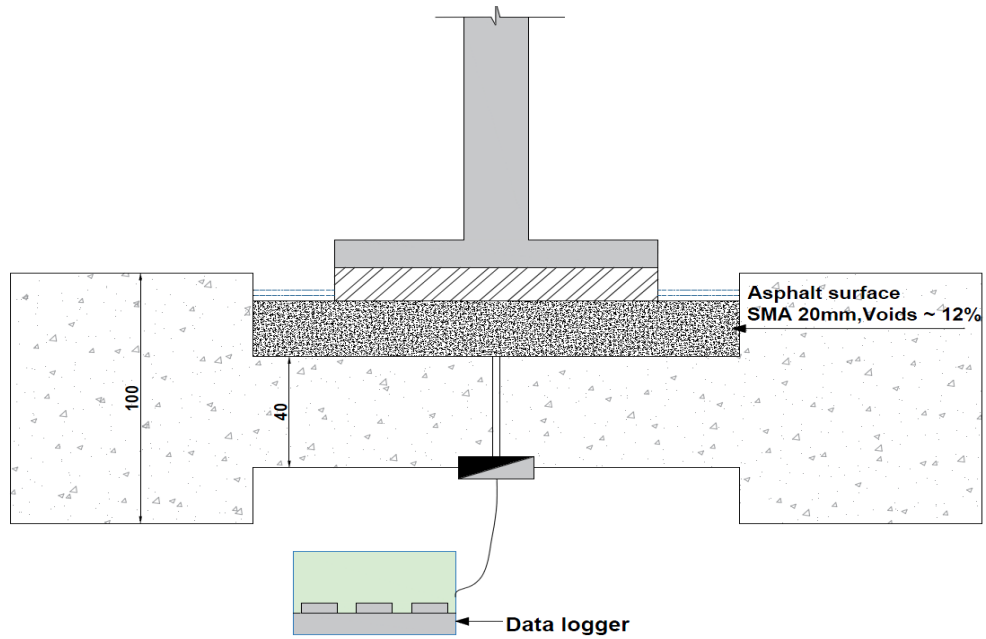
464
465
466

Figure 4b: Idealised pavement with asphalt overlay



467
468
469
470

Figure 5a: Scenario No. 1

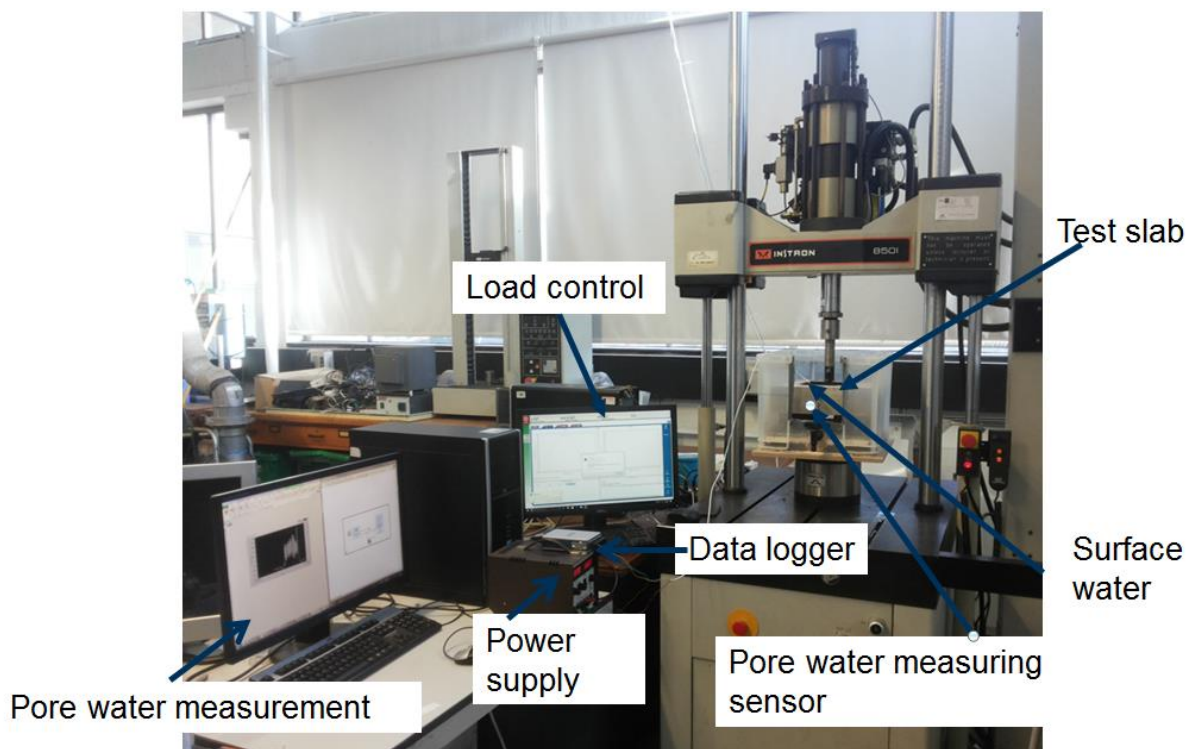


471

472

473

Figure 5b: Scenario No. 2



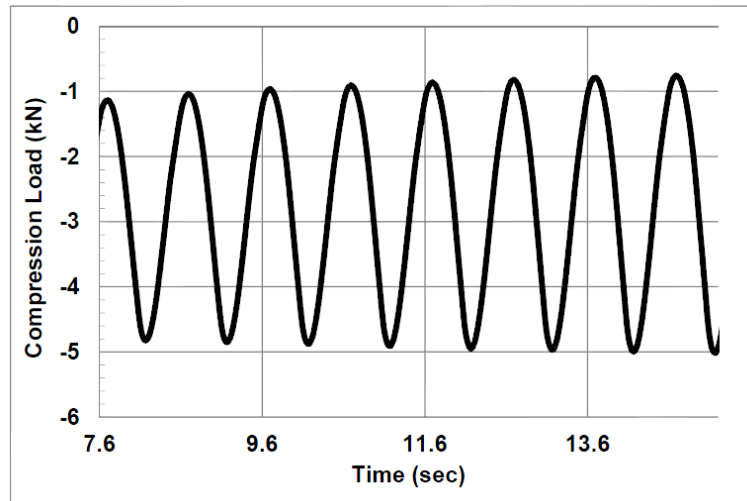
474

475

476

Figure 6. Experimental set-up

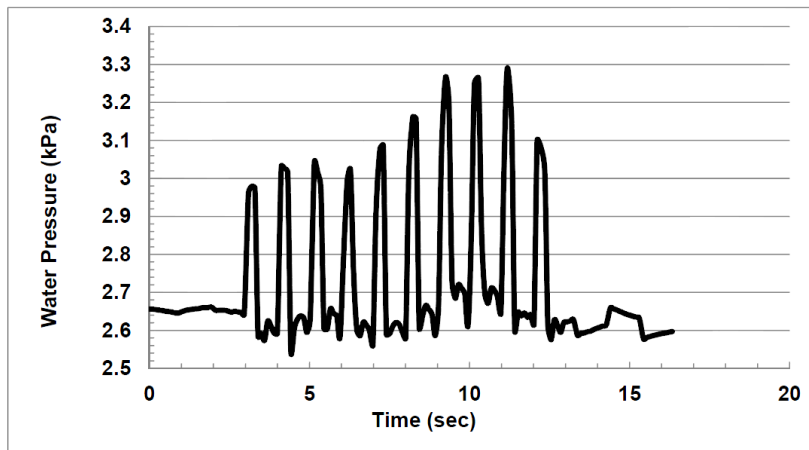
477



478

Figure 7a. Applied load 5kN at 1 Hz

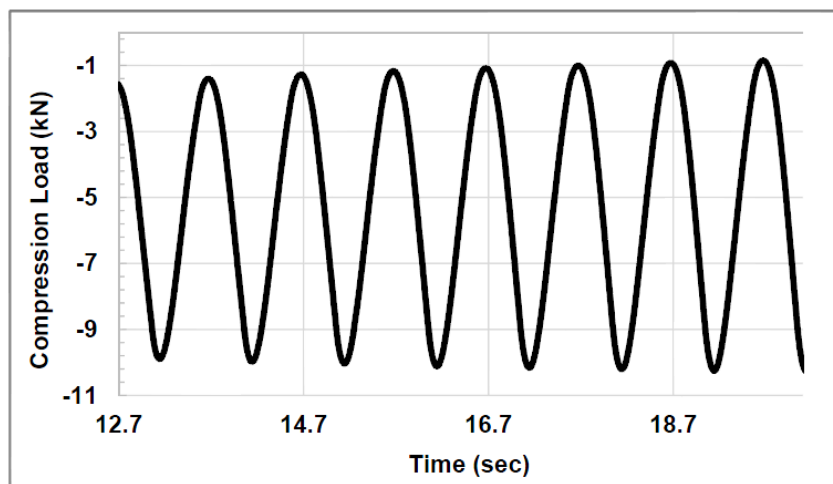
479



480

Figure 7b. Pore water pressure at 5 kN at 1 Hz

481



482

483

484

Figure 7c. Applied load 10kN at 1 Hz

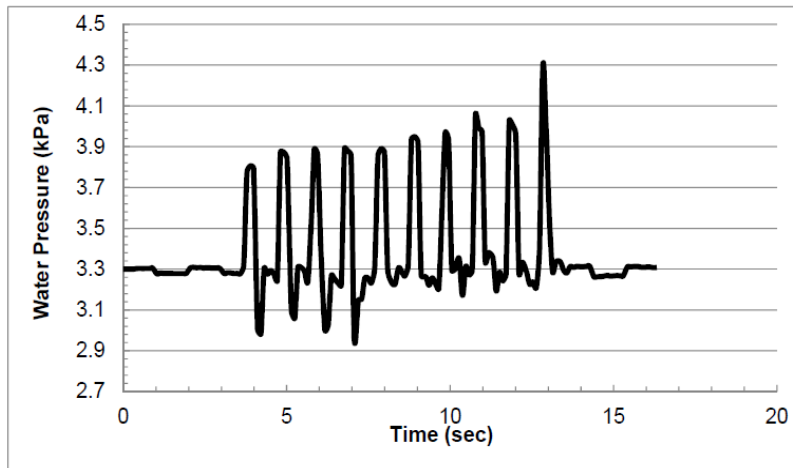


Figure 7d. Pore water pressure at 10 kN at 1 Hz

485
486
487
488
489

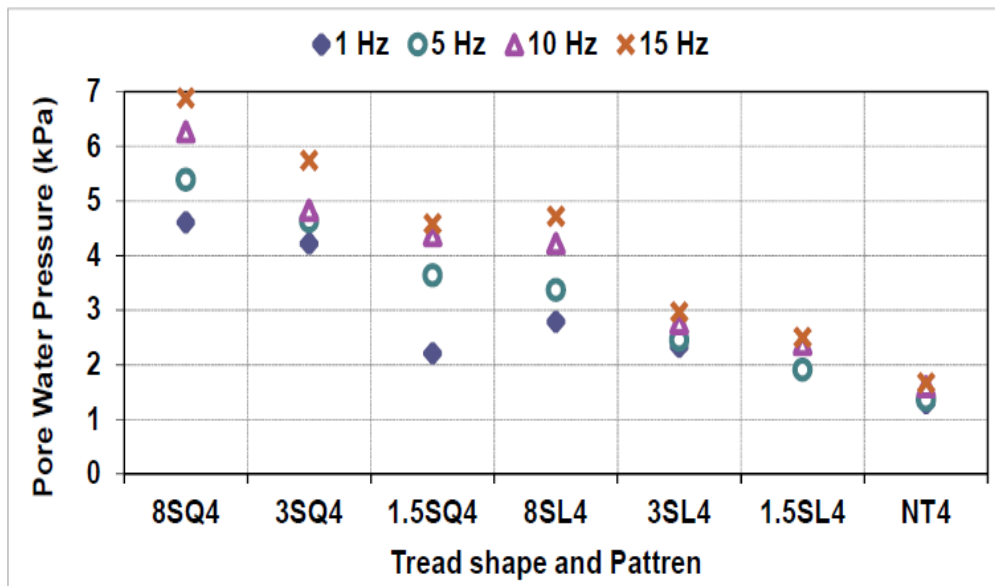
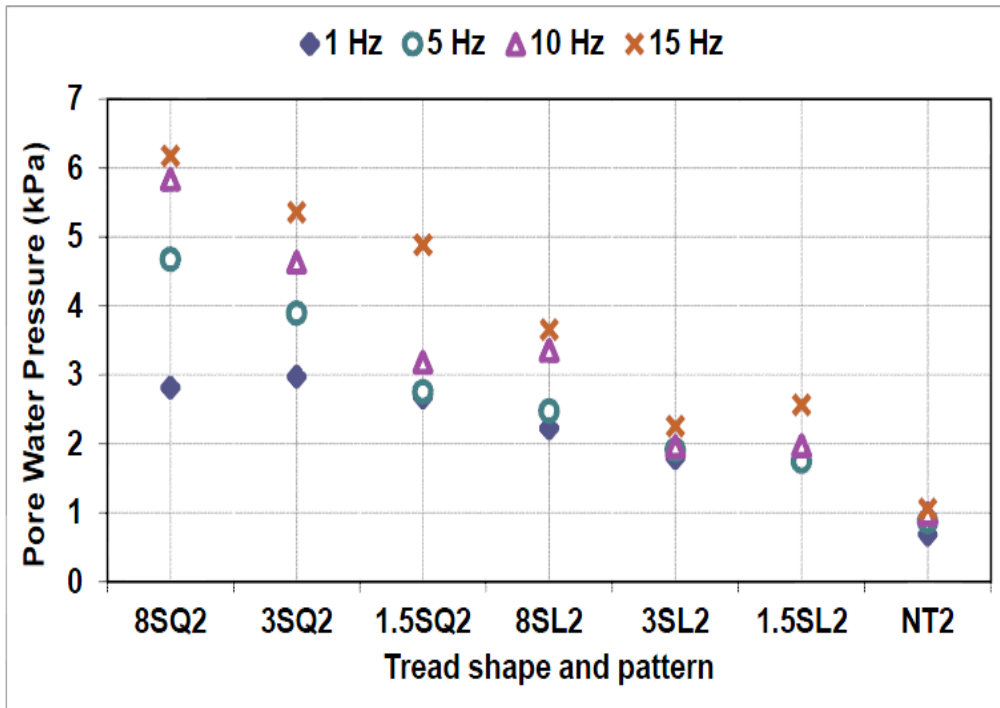


Figure 8a. 4mm surface water, load 5kN, no asphalt surface

490
491
492

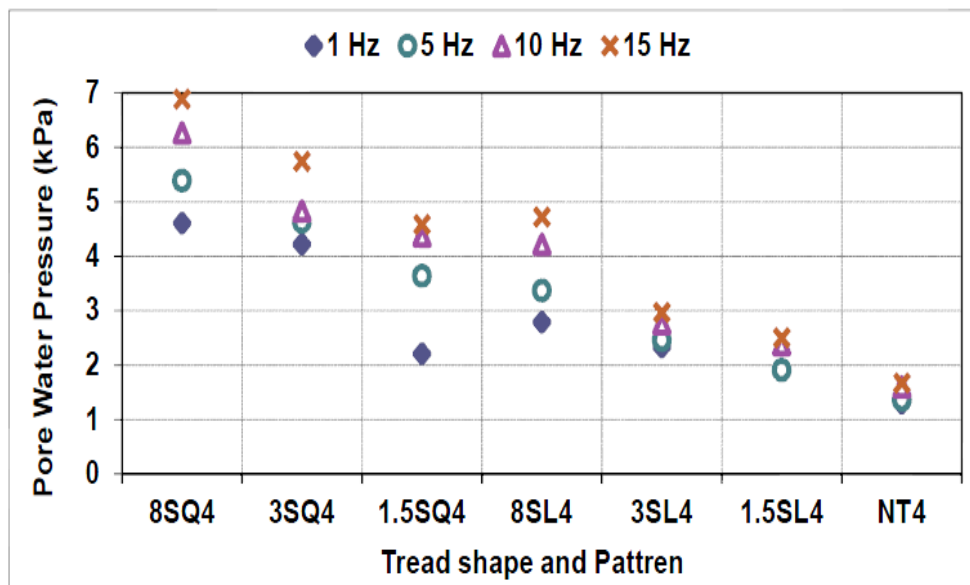


493

494

495

Figure 8b. 2mm surface water, 5 kN load, no asphalt surface

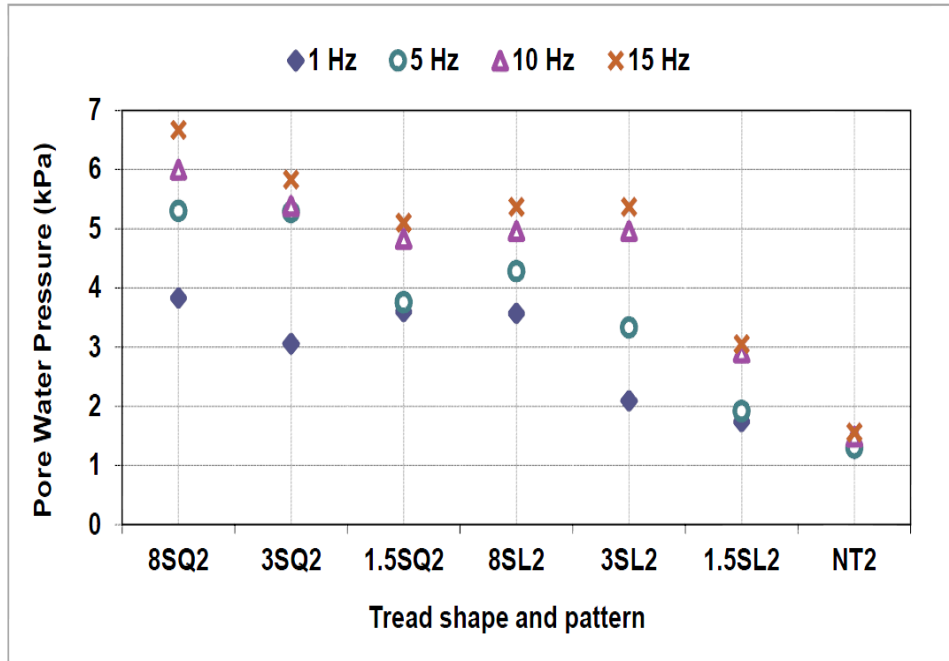


496

497

498

Figure 8c. 4mm surface water, 10kN load, no asphalt surface

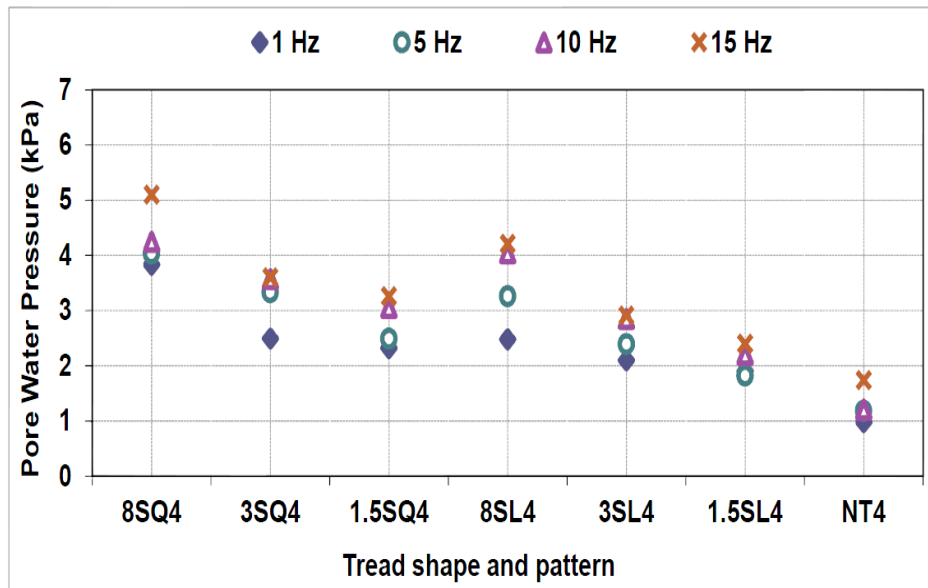


499

500

501

Figure 8d. 2mm surface water, 10kN load, no asphalt surface

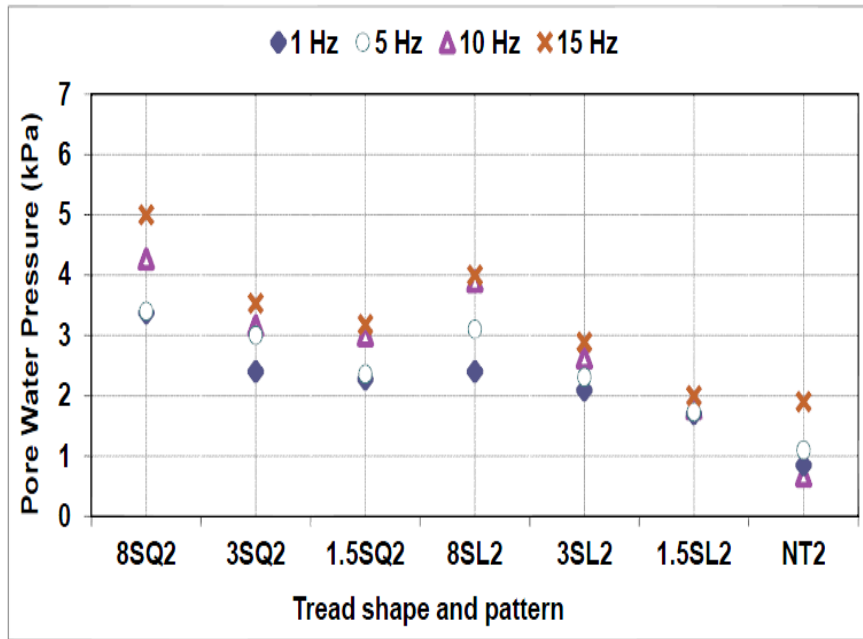


502

503

504

Figure 8e. 4mm surface water, 5kN load, with 20mm asphalt surface

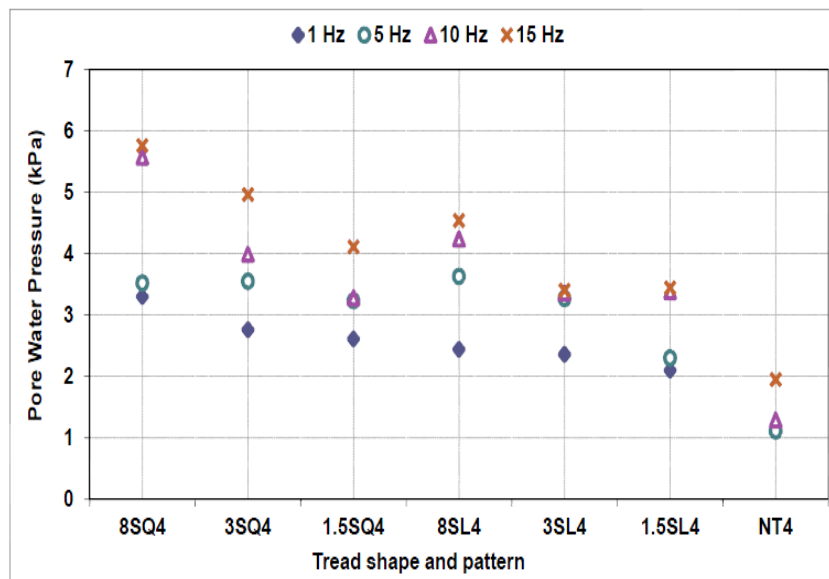


505

506

507

Figure 8f. 2mm surface water, 5kN load, with 20mm asphalt surface

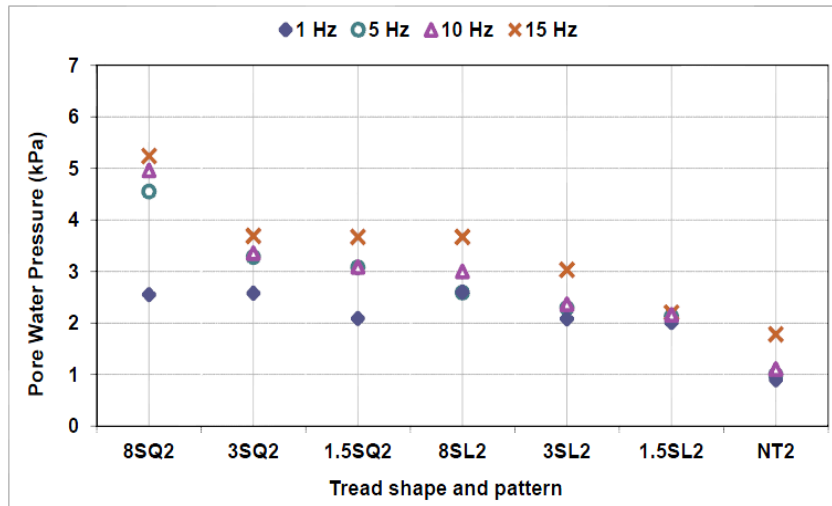


508

509

510

Figure 8g. 4mm surface water, 10kN load, with 20mm asphalt surface



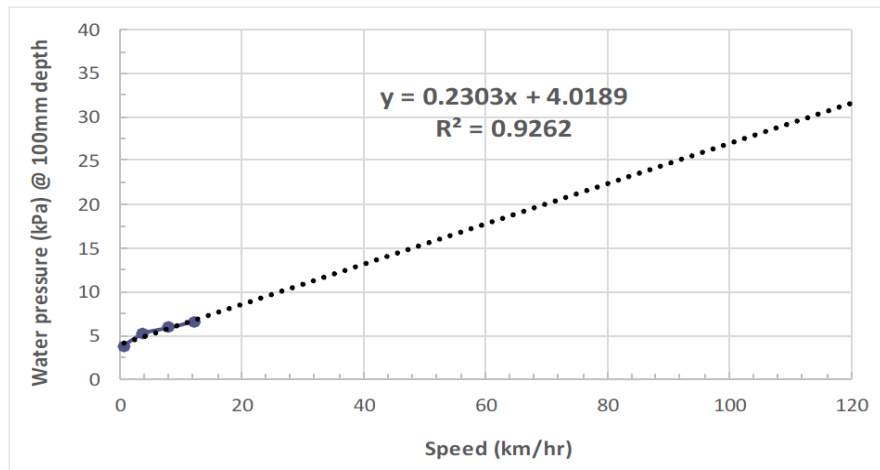
511

512

513

514

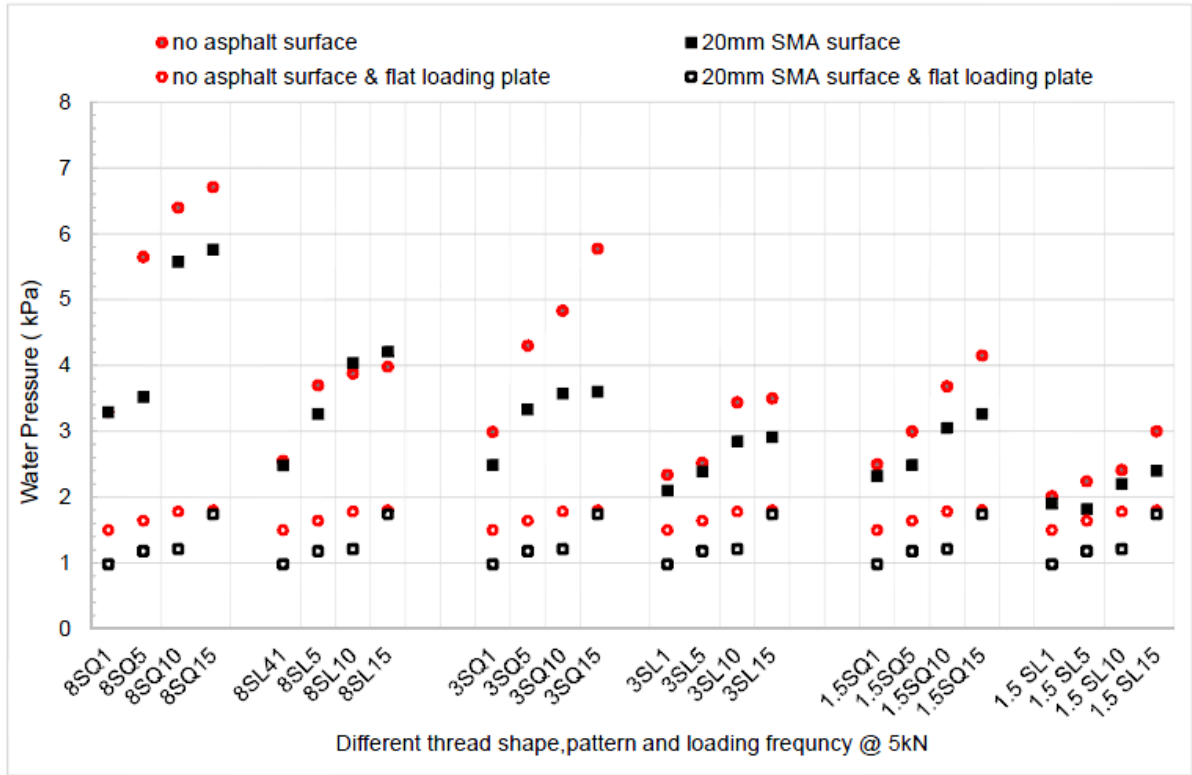
Figure 8h. 2mm surface water, 10kN load, with 20mm asphalt surface



515

516

Figure 9. Extrapolated relation between water pressure and vehicle speed



517

518 **Figure 10.** Comparison of water pressure at different frequencies on pavement with and without asphalt
 519 surface

520